Preventing trogocytosis by cathepsin B inhibition augments CAR T cell function

Kenneth A. Dietze[1], Kiet Nguyen[2], Aashli Pathni[3], Frank Fazekas[2], Jillian M. Baker[1], Etse Gebru[4], Alexander Wang[1], Wenxiang Sun[5], Ethan Rosati[5], David Lum[5], Aaron P. Rapoport[4], Xiaoxuan Fan[1], Djordje Atanackovic[4], Arpita Upadhayaya[2,6,7], Tim Luetkens[1,4]

[1] Department of Microbiology and Immunology, University of Maryland School of Medicine, Baltimore, MD, USA

[2] Biophysics Graduate Program, University of Maryland, College Park, MD, USA

[3] Biological Sciences Graduate Program, University of Maryland, College Park, MD, USA

[4] Department of Medicine and Transplant/Cell Therapy Program, University of Maryland School of Medicine and Marlene and Stewart Greenebaum Comprehensive Cancer Center

[5] Preclinical Research Resource, Huntsman Cancer Institute, Salt Lake City, UT, USA

[6] Institute for Physical Science and Technology, University of Maryland, College Park, MD, USA

[7] Department of Physics, University of Maryland, College Park, MD, USA

One sentence summary: CAR-mediated trogocytosis directly causes CAR T cell exhaustion and fratricide but can be prevented by inhibiting the cysteine protease cathepsin B through overexpression of human cystatins.

Word count (abstract): 189

Word count (main text): 2467

Figures/Tables: 5 Figures, 4 Suppl. Figures, 1 Suppl. Table

Competing Interests Statement: KAD and TL are inventors on U.S. patent application 63/595,007 describing the use of endogenous inhibitors of cathepsin B to augment CAR T cell function. The other authors are not declaring any conflicts of interest.

*Corresponding author:
Tim Luetkens, M.D.
Associate Professor of Microbiology and Immunology
Director R&D at Fannie Angelos Cellular Therapeutics Laboratory
University of Maryland
655 W Baltimore St, RM. 9-009
Baltimore, MD 21201
Phone: 410-706-1924
Email: tluetkens@som.umaryland.edu

ABSTRACT

Chimeric antigen receptor (CAR) T cell therapy has shown remarkable efficacy in cancer treatment. Still, most patients receiving CAR T cells relapse within 5 years of treatment. CAR-mediated trogocytosis (CMT) is a potential tumor escape mechanism in which cell surface proteins transfer from tumor cells to CAR T cells. CMT results in the emergence of antigen-negative tumor cells, which can evade future CAR detection, and antigen-positive CAR T cells, which is hypothesized to lead to CAR T cell fratricide and dysfunction. Using a system to selectively degrade trogocytosed antigen in CAR T cells, we show that the presence of trogocytosed antigen in CAR T cells directly causes CAR T cell fratricide and exhaustion. By performing a small molecule screening using a custom high throughput CMT-screening assay, we identified the cysteine protease cathepsin B (CTSB) as a key driver of CMT. We show that overexpression of cystatin A (CSTA), an endogenous human inhibitor of CTSB, reduces trogocytosis resulting in prolonged antitumor activity and increased CAR T cell expansion/persistence. Overall, we show that targeting CMT is an effective approach to enhance CAR T cell function, which may improve their clinical efficacy.

INTRODUCTION

Chimeric antigen receptors (CAR) are genetically engineered proteins combining antigen binding domains with immune cell activation domains[1–3]. T cells and natural killer (NK) cells engineered to express CARs recognize tumor-associated antigens with high specificity and are clinically effective treatments for patients with hematologic malignancies and autoimmune diseases[1,4–9]. It has previously been shown that CAR T cells and CAR NK cells rapidly transfer the targeted antigen from tumor cells to their own cell surface in a process called trogocytosis[10–12]. CAR-mediated trogocytosis (CMT) is associated with increased expression of apoptotic and exhaustion markers as well as reduced expansion[10–12]. In addition, it has been shown that T cells engineered to express the tumor antigen CD19 are efficiently killed by other CD19 CAR T cells ("fratricide")[10]. Mechanistically linking CMT to exhaustion, fratricide, and reduced CAR T cell expansion has, so far, been elusive due to the lack of specific inhibitors of trogocytosis. Analogously, no approaches exist to inhibit CMT therapeutically to enhance CAR T cell function.

In this study, we develop an analytical framework to explore the mechanistic basis and functional consequences of trogocytosis in CAR T cells. Using this approach, we demonstrate that CAR T cell dysfunction is directly caused by CMT and we identify a genetically encoded, fully-human approach for the persistent suppression of CMT to increase expansion and antitumor activity of CAR T cells.

RESULTS

CAR-mediated trogocytosis directly causes CAR T cell dysfunction

CAR-mediated trogocytosis (CMT) is the extraction of the targeted tumor antigen from the tumor cell surface and its incorporation into the CAR T cell plasma membrane[10–13] (Fig. 1A). *Ex vivo*, CMT occurs across cancer types[10,11] and target antigens, including CD19[10,11], CD22[10], mesothelin[10], and BCMA[13]. We found robust transfer of CD19 to CD19-targeting CAR T cells (clone: FMC63) as well as CD19 loss on tumor cells (Fig. 1B/C), which can be observed just minutes after CAR T cells contact target cells (Fig. 1D, Suppl Fig. S1A). In the clinical setting, CMT had only been shown to occur in B cell lymphoma patients treated with CAR NK cells[12]. By analyzing peripheral blood mononuclear cells (PBMCs) from patients who had recently received CD19 CAR T cells, we observed that CMT also occurs in patients treated with CAR T cells (Fig. 1E/F). The presence of trogocytosed antigen on CAR T cells is correlated with increased exhaustion and reduced viability[10–12] but it remains unknown if CMT is the cause of these effects. We, therefore, developed an approach for the targeted degradation of trogocytosed CD19 fused to GFP (CD19-GFP) in CAR T cells (Fig. 1G). Expression of a trogocytosed antigen degrader (TAD), the Nslmb E3-targeting domain[14,15] fused to a GFP-binding protein (TAD_{GFP}), results in a significant reduction of total and surface CD19 in 293T cells engineered to express CD19-GFP (Suppl Fig. S1B/C). Expression of TAD_{GFP} in CAR T cells did not alter their expansion during manufacturing or their short-term antitumor activity (Suppl Fig. S1D/E).

When cocultured for 2 hours with K562 cells expressing CD19-GFP, unmodified FMC63 CAR T cells showed increased levels of CD19 (Fig. 1H) and GFP (Fig. 1I) indicative of

CMT. When overexpressing TAD_{GFP} in FMC63 CAR T cells, the amounts of CD19 and GFP were significantly reduced in the CAR T cells after coculture (Fig. 1H/I). In addition, TAD_{GFP} expression resulted in significantly increased CAR T cell numbers (Fig. 1M) independent of CAR T cell proliferation (Suppl. Fig. S1F) indicating reduced levels of fratricide. Targeted degradation of trogocytosed antigen was further validated using a fully human TAD (TAD_{CD19}) construct directly targeting CD19. To recognize CD19, TAD_{CD19} uses the Lyn kinase SH2 domain (Fig. 1J), which has been shown to bind the intracellular domain of CD19 with high affinity. Expression of TAD_{CD19} in FMC63 CAR T cells resulted in reductions in CMT comparable to TAD_{GFP} (Fig. 1K/L).

It has previously been shown that the FMC63 CAR can bind to CD19 in *cis*[16]. Following acquisition of CD19 by CMT, $CD19^+$ CAR T cells may therefore experience persistent CAR signaling, which in turn may result in T cell exhaustion (Suppl. Fig. 1G). We found that FMC63 CAR T cells exposed to CD19-GFP^+ K562 cells showed increased expression of exhaustion markers TIM-3 and LAG-3 compared to negative control T cells expressing a CAR without a binding domain (ΔscFv, Fig. 1N). Expression of TAD_{GFP} prevented TIM-3/LAG-3 upregulation demonstrating that increased exhaustion marker expression is the direct consequence of antigen transfer to CAR T cells (Fig. 1N).

CMT-induced fratricide and exhaustion could substantially limit long-term CAR T cell antitumor activity. In a serial coculture stress test of CAR T cell efficacy (Fig. 1O), we found that TAD_{GFP} substantially increased the ability of CAR T cells to control B cell acute lymphoblastic leukemia (B-ALL, Fig. 1P).

These data demonstrate that CMT directly causes CAR T cell dysfunction and fratricide, limiting expansion and antitumor activity.

Extracellular cathepsin B is a key driver of CAR-mediated trogocytosis

Little is known regarding the molecular and cellular drivers of CMT, and to date there are no high-throughput assays to systematically probe potential modulators of CMT as it occurs in real-time. To address this, we developed a luciferase complementation assay for the real-time detection of CMT (CompLuc, Fig. 2A). In this assay, luciferase complementation occurs following the transfer of CD19 fused to the C-terminal fragment of NanoLuc[17] (cLuc) to CAR T cells, which express a complementary N-terminal NanoLuc (nLuc) fragment with high affinity for cLuc (Suppl. Fig. S2A-C). The CompLuc assay allows highly sensitive detection of small numbers of $nLuc^{+}cLuc^{+}$ CAR T cells in cocultures (Suppl. Fig. S2D). We demonstrate that CMT, as quantified by CompLuc, is antigen-dependent and correlates with effector-target ratio (Fig. 2B/C) and flow cytometry endpoint analysis (Fig. 2B). To further validate the CompLuc assay, we determined the effect of an established modulator of CMT, the actin polymerization inhibitor cytochalasin D[10,18]. Treatment of CAR T cells with cytochalasin D significantly reduced CMT in a dose-dependent manner as measured by the CompLuc assay (Fig. 2D).

Using CompLuc, we next investigated the possibility of targeting CMT without altering CAR T cell-mediated tumor cell killing. Actin polymerization inhibitors, including cytochalasin D, significantly limit T cell cytotoxicity (Fig. 2E) but we hypothesized that CMT could be mechanistically distinct from cytotoxic function and could be targeted

selectively. Because it has previously been shown that CMT requires direct cell-to-cell contact[10], we explored the effect of inhibiting various processes at the T cell immune synapse on CMT[10,18–21] (Fig. 2F). We found that inhibition of cathepsin B (CTSB) in FMC63 CAR T cells reduced CMT in a dose-dependent manner as measured by CompLuc (Fig. 2G) without substantially altering CAR T cell cytotoxicity (Fig. 2H). Using a membrane-impermeable inhibitor of CTSB, we found that inhibition of extracellular CTSB is sufficient to prevent CMT (Fig. 2I).

CTSB is a ubiquitously expressed cysteine protease, primarily localized to lysosomal and endosomal compartments under physiological conditions, where it is primarily involved in protein degradation and turnover[22,23]. However, CTSB is also found in the cytosol, retains its catalytic activity at neutral pH[24], and has been shown to line exocytic granules of cytotoxic T lymphocytes[25]. In addition to proteolytic degradation within the endosome and lysosome, CTSB has been implicated in the degradation and remodeling of components of the extracellular matrix, such as collagen and fibronectin, thereby promoting the invasion and metastasis of tumor cells[24,26,27]. Similarly, CTSB may contribute to the extraction of antigen-rich membrane fragments prior to their transfer to CAR T cells.

To determine whether CTSB localizes to the immune synapse upon antigen contact, we generated FMC63 CAR T cells expressing CTSB fused to mCherry. When exposed to immobilized CD19 (Fig. 2J), we found that CTSB in FMC63 CAR T cells, but not ΔscFv CAR T cells, rapidly localized to the immune synapse following CAR T cell antigen recognition (Fig. 2K-M, Suppl. Fig. 1A), correlating with increased trogocytosis as measured by CompLuc and flow cytometry (Fig. 2N).

Taken together, quantification of CMT by CompLuc enabled the identification of extracellular CTSB produced by CAR T cells as a key driver of CMT that is dispensable for CAR-mediated killing. These data indicate that CTSB is a potential therapeutic target to prevent trogocytosis and thereby improve CAR T cell efficacy.

Expression of human cystatins increases CAR T cell expansion by preventing CTSB-mediated CMT.

To date there are no clinically approved small molecule inhibitors of CTSB, and its systemic inhibition may result in substantial toxicities due to the ubiquitous expression of CTSB[28]. Cystatin A (CSTA), a cysteine protease inhibitor in the cystatin superfamily[29], is an endogenous human inhibitor of CTSB[30]. Similar to Ca-074-Me, CSTA prevents access to the active-site cleft of CTSB through insertion of a hydrophobic wedge[31] (Fig. 3A). We hypothesize that overexpression of CSTA in CD19 CAR T cells may selectively and efficiently reduce CMT by inhibiting CTSB (Fig. 3B).

Stable overexpression of CSTA in FMC63 CAR T cells (CAR_{CSTA}) resulted in significantly increased amounts of CSTA (Fig. 3C) and reduced CTSB activity (Fig. 3D). CAR_{CSTA} cells showed equivalent expansion (Fig. 3E), phenotype (Fig. 3F), and short-term antitumor activity (Fig. 3G) compared to conventional FMC63 CAR T cells. We observed significantly reduced CMT in these cells as measured by CompLuc (Fig. 3H/I). CMT was similarly reduced when overexpressing the closely related superfamily member cystatin B[32] or a truncated variant of CSTA ($CSTA_{1-57}$) containing the hydrophobic wedge (Suppl. Fig. S3A-D). CSTA overexpression reduced both antigen transfer to CAR T cells (Fig. 3K, Suppl. Fig. S3F) and antigen loss on tumor cells (Fig.

3J, Suppl. Fig. S3E), suggesting inhibition of CMT at the antigen extraction step. This CSTA-mediated inhibition of CMT resulted in significantly increased CAR T cell expansion when exposed to tumor cells (Fig. 3L, Suppl. Fig. S3G). Taken together, these data demonstrate that inhibition of CTSB through overexpression of human CSTA significantly reduces CMT and improves CAR T cell expansion *in vitro*.

Cystatin overexpression improves long-term CAR T cell expansion and efficacy

We have shown that CMT drives CAR T cell exhaustion and fratricide resulting in reduced CAR T cell numbers and potentially affecting the cells' long-term antitumor activity. To explore this, we assessed CAR_{CSTA} T cell persistence and antitumor activity in an extended serial coculture model (Fig. 4A). We observed significantly higher numbers of CAR_{CSTA} T cells over time (Fig. 4B) despite no differences in activation (Fig. 4C) or proliferation (Fig. D), indicating that CSTA overexpression results in improved expansion, likely driven by reduced fratricide. In addition, we observed that CAR_{CSTA} T cells exhibit superior long-term *in vitro* tumor control (Fig. 4E). Similarly, we observed significantly increased *in vivo* CAR_{CSTA} T cell expansion (Fig. 4F/G).

Cystatin A CAR T cells show reduced trogocytosis in a BCMA CAR T cell model

CMT has previously been shown to occur across cancer types and target antigens[10,13]. In addition to CD19, the FDA has approved two CAR T cell products targeting B cell maturation antigen (BCMA) for the treatment of multiple myeloma[4,5,33,34] (Fig. 5A). We found that, like FMC63 CAR T cells, BCMA CAR T cells are subject to CMT as BCMA is transferred to CAR T cells (Fig. 5B). In addition, we observed BCMA loss on multiple

myeloma cells when cocultured with both FDA-approved CAR T cell products (Fig. 5C). We next assessed whether CSTA overexpression is able to prevent BCMA-specific CMT. As observed for CD19 CAR T cells, CSTA expression in BCMA CAR T cells did not alter CAR T cell expansion during manufacturing (Fig. 5D) or their phenotype (Fig. 5E). BCMA CAR_{CSTA} T cells showed slightly improved short-term antitumor activity against multiple myeloma cell lines (Fig. 5F) and increased expansion at the end of the coculture (Fig. 5G) compared to conventional BCMA CAR T cells. Following exposure to K562 cells overexpressing a BCMA-GFP fusion protein, BCMA CAR_{CSTA} T cells exhibited significantly reduced CMT as measured by CompLuc (Fig. 5H/I) and flow cytometry (Fig. 5J/K, Suppl. Fig. 4A/B), resulting in increased CAR T cell expansion (Fig. 5L).

These data indicate that CSTA overexpression is an effective approach to reduce CMT across target antigens and to increase CAR T cell expansion.

DISCUSSION

CAR T cells have revolutionized cancer immunotherapy, but most patients receiving CAR T cell therapy relapse within 5 years of treatment[35–37]. Several mechanisms of CAR-mediated relapse have been described, including CAR T cell-mediated trogocytosis (CMT). CMT affects CAR T cell function in three key ways: 1) by rendering tumor cells temporarily antigen negative, 2) by causing CAR T cells to be killed by other CAR T cells, and 3) by inducing exhaustion, potentially through CAR binding tumor antigen in cis, leading to persistent CAR signaling[10–12]. Previous studies have demonstrated the presence of tumor antigen on CAR T cells following tumor cell cocultures and that the presence of trogocytosed antigen was correlated with increased apoptotic markers and exhaustion[10,11]. However, it had remained unknown if the two were caused by CMT.

In this study, using targeted degradation of trogocytosed antigen-GFP fusion proteins, we now causally link CMT to CAR T cell fratricide and exhaustion. We also demonstrate that the trogocytosed antigen degrader (TAD) approach can be adapted to degrade antigens by using endogenous protein domains binding to the target antigen's intracellular domain. Further work will be needed to explore target specificity/orthogonality of such endogenous binding domains to ensure CAR T cell functionality. Additionally, using small molecule- and protein-based inhibitors, we show that the cysteine protease cathepsin B (CTSB) produced by CAR T cells is essential for CMT. When expressed in tumor cells, extracellular CTSB has been shown to contribute to the metastatic process by degrading and remodeling components of the extracellular matrix [24,26,27]. Analogously, our data show that CTSB produced by CAR T cells rapidly

localizes to the immune synapse and that CMT, specifically antigen extraction from tumor cells, is conferred by extracellular CTSB. To develop an approach to specifically inhibit CMT in CAR T cells, we explored the overexpression of cystatins belonging to the stefin family, established inhibitors of cathepsins[29,31]. We found that both cystatin A and cystatin B potently inhibited CTSB in CAR T cells. While the small molecule inhibitors used throughout this study have been shown to be specific for CTSB [38,39], the more robust inhibition of CMT by cystatins could also indicate a role of other cathepsins, such as cathepsin L and H in CMT[29,31]. Future work will be needed to further delineate the precise molecular mechanism by which extracellular CTSB and potentially other cathepsin proteins are able to confer antigen extraction from tumor cells.

Our study focused on CAR T cell approaches targeting the two clinically validated CAR T cell antigens CD19 and BCMA approved for the treatment of several hematologic malignancies. However, we propose that future work should include an in-depth exploration of CMT in solid malignancies. In this setting, exhaustion-driven T cell dysfunction is generally more pronounced [40,41] and CMT may play a key role. In addition, a denser tumor microenvironment and constrained T cell mobility may favor more extensive intratumoral fratricide.

In conclusion, we show that CMT directly causes CAR-mediated fratricide and exhaustion, and that CMT can be mitigated by inhibition of CTSB using overexpression of human endogenous cystatins. Inhibition of CMT in turn results in prolonged antitumor activity and increased CAR T cell persistence.

METHODS

Study approval

All recombinant DNA and biosafety work was approved by the institutional biosafety committees at University of Maryland, Baltimore (protocol IBC-6040). Animal experiments were approved by the institutional animal care and use committee at the University of Utah (protocol 18-1104).

Cell lines and primary human cells

Raji, NALM6, Daudi, DB, Toledo, MM.1S, RPMI8226, U266B1, K562, and Phoenix-AMPHO cells were purchased from the American Type Culture Collection (ATCC) and cultured according to ATCC instructions. Lenti-X 293T cells were purchased from Takara and cultured according to the manufacturer's instructions. Cell lines were authenticated by their respective supplier. Healthy donor buffy coats were obtained from the New York Blood Center. PBMCs from healthy donors were isolated from buffy coats by density gradient using FicollPaque (GE) as previously described[34,42]. Primary human T cells were cultured in AIM-V medium (Invitrogen 12055-083) supplemented with 5% Human serum (Sigma H4522-100ML), 1% Pen/Strep (Thermofisher 15140-122) (T cell media), and 40 IU IL-2 (R&D Systems #202-IL-10). All cells were cultured at 37°C, 5% CO2.

Vector constructs

All vectors generated for this study were produced by Twist Biosciences. FMC63-nLuc contains the CD19-specific scFv fragment FMC63 [43]. All CAR constructs contain the CD8α hinge/transmembrane domain, 4-1BB costimulatory domain, and CD3z domain.

For some constructs, the full-length sequence of human cystatin A (UniProt, P01040) was synthesized and cloned downstream of the respective CAR and nLuc fragment separated by a P2A sequence (Twist Bioscience). DNA was isolated using Endofree Plasmid Maxi Kit (Qiagen 12362) following the manufacturer's protocol. Plasmid concentration was measured using a NanoDrop One instrument (Thermo). All DNA constructs were stored at -20°C.

Clinical data

Whole blood was drawn from patients receiving CAR T cell therapy 7-28 days after CAR T cell injection. Peripheral blood mononuclear cells (PBMCs) were isolated by density gradient using Ficoll Paque as previously described[34,42]. PBMCs were stained with anti-hCD3, anti-hCD4, anti-hCD8, anti-CAR, and anti-hCD19, anti-hCD27, anti-hCD137, and 7-AAD and analyzed by flow cytometry. Samples were collected under Institutional Review Board (IRB)-approved protocol 2043GCCC (IRB H0091736, PI: D. Atanackovic).

Gammaretrovirus Production

Gammaretrovirus was produced using Phoenix-AMPHO cells (ATCC, catalog no. CRL-3213). Phoenix-AMPHO cells were transiently transfected with 16 µg of plasmid DNA using Opti-MEM Reduced Serum Medium (Thermofisher, catalog no. 31985070) and lipofectamine 2000 (Invitrogen 11668-019) according to manufacturer's instructions. During transfection, cells were cultured in Dulbecco's Modified Eagle Medium (DMEM, Thermofisher 11995073) supplemented with 10% FBS. Virus-containing supernatant was filtered using Steriflip™ Sterile Disposable Vacuum Filter Units (Millipore Sigma

SEIM003M00). Virus was concentrated using Retro-X Concentrator (Takara, 631456). The following day, concentrated virus was centrifuged at 1500 x g for 45 minutes at 4°C. Supernatant was removed and concentrated virus was resuspended in 1.5 mL complete T cell media.

Transgenic T cell production and expansion

CAR T cells were generated as previously described[11,34,42]. Buffy coats from healthy donors were obtained from the New York Blood Center and peripheral blood mononuclear cells (PBMCs) were isolated using Ficoll-Paque and cryopreserved until use. PBMCs were thawed and cultured overnight in complete T cell media. PBMCs were stimulated for 2 days with anti-CD3/anti-CD28 T cell activation beads (Thermo, catalog no. 11131D) in the presence of interleukin-2 (IL-2; 40 IU/ml; R&D Systems, catalog no. 202-IL-010) in complete T cell media and incubated at 37°C, 5% CO_2. Bead-stimulated cells were transferred to RetroNectin-coated (Takara) virus–containing plates and incubated overnight. Transduction was repeated the next day before counting and diluting cells to 0.4×10^6 cells/ml. After the second transduction, cells were grown for an additional 7 days before removing beads using a DynaMag-15 magnet (Thermo Fisher Scientific). IL-2 was replenished every 2 days to 40 IU/ml. Cells were frozen in 90% fetal bovine serum/10% dimethyl sulfoxide and stored in liquid nitrogen. CAR T cell transduction efficiency and phenotype were determined by flow cytometry. CAR T cells were washed with FACS buffer and stained with antibodies targeting hCD3, HA, hCD4, hCD8, hCD95, hCD62L, and hCD45RA.

Imaging Substrate Preparation

Eight-well chambers (Cellvis, catalog no. C8-1.5H-N) were used for all experiments. For CAR T cell activation on CD19-coated surfaces, 8-well chambers were coated with 0.01% poly-L-lysine (PLL) solution diluted in distilled water for 10 minutes at room temperature. PLL was aspirated from each well, and the chambers were allowed to air-dry for 1 hour at 37°C. PLL-coated dishes were then incubated overnight at 4°C with a 10 µg/mL solution of NeutrAvidin (Thermo Scientific, catalog no. 31000) in 1x Dulbecco's phosphate-buffered saline (DPBS). After overnight incubation, coated wells were washed with 1x DPBS at room temperature and incubated at 37°C with a 10 µg/mL solution of biotinylated human CD19 protein (ACRO Biosystems catalog no. CD9-H82E9) in DPBS for 2 hours at 37°C. Prior to the experiment, coated wells were washed three times with RPMI 1640 phenol red-free imaging medium. For coculture experiments, 8-well chambers wells were incubated with 10 µg/mL fibronectin (MilliporeSigma, catalog no. 34-163-11MG) in DPBS at room temperature for 1 hour prior to seeding with 293T cells stably expressing CD19-GFP. 293T cells were seeded at a concentration of 5 x 10^5 cells per well in complete growth media, followed by an overnight incubation at 37°C, 5% CO_2. Prior to imaging, wells were washed three times with warm complete imaging media, consisting of a 1:1 ratio of RPMI 1640 supplemented with 5% fetal bovine serum (FBS) and DMEM supplemented with 10% FBS. The washing process was performed thrice to ensure removal of any residual media while leaving a known volume in the wells.

Confocal Microscopy

Confocal microscopy was conducted using an inverted microscope (Nikon Ti-E PFS, Nikon Inc.) equipped with a 100× Silicone objective lens. Imaging was performed with a

Prime BSI camera (Photometrics). Image acquisition protocols were managed using Nikon Elements software, and images were cropped in FIJI for further analysis. All live cell imaging was done with imaging chambers placed in a stage-top Okolab Incubator (Okolab S. R. L.) pre-equilibrated to 37°C with 5% CO_2. For live cell imaging on glass, activated CAR T cells suspended in RPMI 1640 medium supplemented with 5% FBS were deposited onto CD19-coated surfaces. Imaging was started between 3 to 6 minutes after CAR T cells expressing CTSB-mCherry were added to a biotin-CD19-coated coverslip. For each well, timelapse images of a 3D volume (planes with z spacing of 0.3 µm to span the cell from the top to the bottom) were acquired every 3 minutes for 60 minutes. For coculture experiments, imaging was started between 3 to 6 minutes after CAR T cells expressing CTSB-mCherry were dropped onto a layer of 293T cells expressing CD19-GFP seeded on a coverslip, at a concentration of 7×10^4 cells per drop. Brightfield imaging was used to identify cells attached to the apical surface of HEK293 cells. The synaptic plane between a CAR-T cell and a HEK293 cell was identified and designated as the home plane for acquisition of Z-stack time-lapse movies. Two-channel images using 488 nm and 561 nm lasers (for GFP and mCherry imaging respectively) were acquired every 3 minutes for 1 hour and 15 minutes utilizing a Z-spacing of 0.3 or 0.6 µm, with brightfield images taken at the home plane.

Image analysis was carried out in MATLAB (Mathworks, Inc.) using custom scripts. The plane of the synapse was determined using the actin channel. After background subtraction, axial intensity gradients are estimated for every voxel of sufficient intensity within the ROI. Below the cell, these gradients are typically positive due to the Airy

pattern of the PSF. The synapse is taken as the first plane for which the gradients are no longer consistently positive.

Estimating the average distance of CTSB to the synapse

The center of fluorescence (COF) of CTSB is defined similarly to the center of mass. The voxel positions are weighted by CTSB intensity after background subtraction and thresholding to obtain the COF. The average CTSB distance is then calculated from the axial (z) distance of the Cathepsin B COF to the plane of the synapse.

Characterizing CTSB axial dispersion

The axial dispersion is an estimate of the average distance of CTSB molecules to the COF. The axial (z) distance of each voxel to the COF is determined, and the axial dispersion is defined as the average of these distances weighted by CTSB intensity after background subtraction and thresholding. Voxels with sufficiently low signal do not contribute to the calculation due to the thresholding procedure.

CTSB clustering at the synapse

The pair auto-correlation function g(r) of CTSB is computed at the synapse using the actin channel as a mask[44]. The actin channel is segmented by smoothing with a Gaussian filter, generating an initial mask by applying k-means clustering (k = 2) after a log transformation, and then applying morphological operations to connect and smooth the initial mask. The clustering coefficient, g_{ave}, is computed by averaging over all radial bins with 0.25 m or 0.5 m.

CompLuc-based trogocytosis assay

Transduced, cryopreserved nLuc+ CAR T cells were thawed and cultured in complete T cell media supplemented with 40 IU IL-2 for 48 hours prior to use. nLuc-expressing CAR T cells were cocultured with CD19-cLuc-expressing K562 tumor cells at the specified effector-target ratios. CAR T cells and tumor cells were resuspended in Opti-MEM reduced serum media. Live Cell Substrate (Promega, catalog no. N2011) was prepared according to manufacturer's instructions. K562 tumor cells and prepared Live Cell Substrate were added to wells of a black 96-well plate and luminescence was measured to assess baseline luminescence. CAR T cells were added to appropriate wells and luminescence was measured every minute for three hours at 37˚C. Luminescence was measured using a Spark multi-mode plate reader (Tecan).

Flow cytometry-based trogocytosis assay

A flow-cytometry based trogocytosis assay was used to confirm results observed in CompLuc, to assess CD19 levels on CAR T cells and tumor cells, and to quantify CAR T cells. 2 x 10^5 target cells were seeded in wells of a 96-well round bottom plate. Various ratios of CAR T cells were cocultured with target cells for 1 hour at 37˚C, 5% CO_2. Following coculture, cells were resuspended by gentle pipetting and transferred to wells of a 96-well V bottom plate for washing and staining. Cells were stained with Zombie violet fixable viability dye, and antibodies for hCD3, HA, and hCD19. Accucheck counting beads (Life Technologies) were added to the cells. Samples were acquired on an LSR II flow cytometer (BD) or an Aurora full-spectrum flow cytometer (Cytek).

Luciferase-based cytotoxicity assay

To determine *in vitro* CAR T cell cytotoxicity, cell lines (Raji, NALM6, Daudi, Toledo) were transduced with pHIV-Luc-ZsGreen lentivirus and sorted on a FACS Aria flow

cytometer (BD) for GFP expression. 3 x 10^4 target cells were seeded in wells of a 96-well round bottom plate. CAR T cells were cocultured with target cells at the indicated effector-target ratios and incubated for 16 hours at 37˚C, 5% CO_2. Following incubation, 80 µL of supernatant was harvested from each well. Cells were suspended by gentle pipetting, and 100 µL was transferred to a 96-well black flat bottom plate. D-Luciferin (Gold Biotechnology, catalog no. LUCNA-2G) at 150 µg/ml was added to the cells and incubated for 5 minutes at 37°C. Luminescence was determined on a Spark multimode plate reader (Tecan).

Serial coculture repeat stimulation assay

To determine the long-term *in vitro* control and exhaustion of CAR T cells, luciferase-expressing tumor cells were plated at 3 x 10^4 cells/well. CAR T cells were cocultured at a defined effector-target ratio and incubated for 24 hours at 37˚C, 5% CO_2. Following incubation, cells were transferred to a 96-well black flat bottom plate. D-luciferin was added to cells and luminescence was determined on a Spark multimode plate reader (Tecan). Next, remaining CAR cells were pooled together and normalized based on expansion. CAR T cells were redistributed to wells and fresh tumor cells were added to each well. Plates were incubated for 48 hours at 37˚C, 5% CO_2. Luminescence measurements and normalization were repeated until a loss of cytotoxicity was observed.

Cystatin A enzyme-linked immunosorbent assay

Cystatin A concentration was assessed using a Human Cystatin A ELISA kit (Invitrogen, catalog no. EH140RB). Total cell lysates were extracted from CAR T cells using radioimmunoprecipitation assay (RIPA) buffer (Thermo) containing protease inhibitor

cocktail (Roche). Total protein concentration was determined using Pierce BCA assay (Thermo). Cystatin A levels were determined by enzyme-linked immunosorbent assay (ELISA) according to manufacturer's instructions (Invitrogen) and calculated using standard curve interpolation. Absorbance was measured at the recommended wavelength on a Spark multimode plate reader (Tecan).

Cathepsin B activity assay

Cathepsin B activity was assessed using the InnoZyme Cathepsin B Activity Assay Kit (MilliPore Sigma, catalog no. CBA001). Total cell lysates were extracted from CAR T cells using the provided cell lysis buffer according to manufacturer's instructions. Total protein concentration was determined using Pierce BCA assay (Thermo Fisher Scientific). Cathepsin B activity was determined fluorometrically according to manufacturer's instructions (Calbiochem). Fluorescence was measured on a Spark multimode plate reader (Tecan).

Treatment of CAR T cells with inhibitors

FMC63 CAR T cells were treated with small-molecule inhibitors targeting Actin (inhibitor: Cytochalasin D, Sigma Aldrich catalog no. C8273), Dynamin (inhibitor: DynaSore, Sigma Aldrich catalog no. D7693), Cathepsin B (inhibitor: Ca-074-Me, SelleckChem catalog no. S7420), Clathrin (inhibitor: PitStop, Abcam catalog no. ab120687), or LFA-1 (inhibitor: BI-1950, Boehringer Ingelheim) at the indicated concentrations for one hour. Following treatment, cells were washed with T cell media and centrifuged at 400 x g for 5 minutes. To determine the effect of the non-membrane permeable CTSB inhibitor CA-074 (Millipore Sigma, catalog no. 205530), the inhibitor was added directly to the co-culture at the indicated concentrations. As a control, CAR T

cells treated with DMSO. CAR T cells were cocultured with CD19-expressing tumor cells for the indicated intervals.

Western blot

Total cell lysates were extracted from CAR T cells using radioimmunoprecipitation assay (RIPA) buffer (Thermo Fisher Scientific) containing protease inhibitor (Roche). Total protein concentration was determined using Pierce BCA assay (Thermo Fisher Scientific). Samples were separated by SDS–polyacrylamide gel electrophoresis, and separated proteins were transferred to nitrocellulose membranes using an iBlot2 transfer system (Thermo Fisher Scientific). Membranes were blocked with 5% nonfat milk–tris-buffered saline and incubated with primary antibodies against CD19 or β-actin. Membranes were washed and developed using species-specific secondary anti-IgG/horseradish peroxidase antibodies (R&D Systems) and Western Lightning Plus-ECL solution (PerkinElmer). Bands were visualized and quantified on an iBright 1500 imaging system (Thermo Fisher Scientific).

In vivo cystatin A model of CAR T cell expansion

6–8-week-old male NRG mice (Jackson Laboratory) were irradiated with a sublethal dose of 200 cGy (Day -1). The next day (Day 0), mice were injected with 4 x 10^5 NALM6 tumor cells via tail vein injection. On Day 4, mice were injected with 1 x 10^6 FMC63 CAR T cells ± Cystatin A overexpression or CAR T cells lacking a binding domain (ΔscFv) via tail vein injection. Animals were weighed twice weekly and monitored for signs of distress in accordance with institutional regulations. On day 28, animals were euthanized and tissues collected for analysis by flow cytometry.

Statistical Analysis

The respective statistical tests are stated in the figure legends. Generally, statistical significance between two groups was determined by two-sided Student's *t*-test or Mann-Whitney U test. Statistical significance between groups of three or more was determined by one- or two-way analysis of variance (ANOVA). Significance of differences between cell numbers, mean fluorescence intensity, and area under curve, was calculated by two-sided Student's *t* test. Significance of differences in murine tumor control was determined by two-way ANOVA. All statistical tests were performed using Prism 10 (GraphPad). Results were considered significant when $p < 0.05$.

ACKNOWLEDGEMENTS

The authors thank the Flow Cytometry Shared Service of the University of Maryland Marlene and Stewart Greenebaum Comprehensive Cancer Center for help with sorting cells and panel design. The authors also thank the Huntsman Cancer Institute at the University of Utah for the use of the Preclinical Research Resource (PRR). This work was supported by funds through the Maryland Department of Health's Cigarette Restitution Fund Program (CH-649-CRF), the National Cancer Institute Cancer Center Support Grant (P30CA134274), the National Institutes of Health to AU (R35 GM145313), and by an NIAID-funded predoctoral fellowship to JMB (T32 AI095190). The plasmid pHIV-Luc-ZsGreen was a gift from Dr. B. Welm (Addgene #39196). The plasmid SFG.CNb30_opt.IRES.eGFP was a gift from Dr. M. Pule (Addgene #22493).

AUTHOR CONTRIBUTIONS

KAD and TL conceived the project, planned and performed experiments, analyzed data, and wrote the manuscript. KAD performed the majority of the described in vitro experiments, generated all transgenic T cells, developed the CompLuc assay, identified and validated the role of CTSB in CMT, and developed the CSTA-based approach of CMT inhibition in CAR T cells. KN and AP performed confocal microscopy and fixed coculture staining and imaging. JMB planned experiments, analyzed data, and edited the manuscript. EG performed CAR T cell phenotyping and analyzed data. FF wrote analysis scripts for CTSB dispersion. WS, ER, and DL planned and performed in vivo models and analyzed data. XF developed full-spectrum flow cytometry panel and performed flow cytometry analysis. AW planned experiments and analyzed data. DA

supervised CAR T cell phenotyping. AU planned and supervised microscopy experiments and analyzed data. TL supervised all work related to this project. All authors reviewed and approved the manuscript.

REFERENCES

1. Sadelain, M. CD19 CAR T Cells. *Cell* **171**, 1471 (2017).
2. Maude, S. L. *et al.* Tisagenlecleucel in Children and Young Adults with B-Cell Lymphoblastic Leukemia. *N. Engl. J. Med.* **378**, 439–448 (2018).
3. Sadelain, M., Rivière, I. & Riddell, S. Therapeutic T cell engineering. *Nature* **545**, 423–431 (2017).
4. Raje, N. *et al.* Anti-BCMA CAR T-Cell Therapy bb2121 in Relapsed or Refractory Multiple Myeloma. *N. Engl. J. Med.* **380**, 1726–1737 (2019).
5. D'Agostino, M. & Raje, N. Anti-BCMA CAR T-cell therapy in multiple myeloma: can we do better? *Leukemia* **34**, 21–34 (2020).
6. Romanski, A. *et al.* CD19□CAR engineered NK□92 cells are sufficient to overcome NK cell resistance in B□cell malignancies. *J. Cell. Mol. Med.* **20**, 1287–1294 (2016).
7. Boissel, L. *et al.* Retargeting NK-92 cells by means of CD19- and CD20-specific chimeric antigen receptors compares favorably with antibody-dependent cellular cytotoxicity. *OncoImmunology* **2**, e26527 (2013).
8. Mackensen, A. *et al.* Anti-CD19 CAR T cell therapy for refractory systemic lupus erythematosus. *Nat. Med.* **28**, 2124–2132 (2022).
9. Mueller, F. *et al.* CD19-Targeted CAR-T Cells in Refractory Systemic Autoimmune Diseases: A Monocentric Experience from the First Fifteen Patients. *Blood* **142**, 220 (2023).
10. Hamieh, M. *et al.* CAR T cell trogocytosis and cooperative killing regulate tumour antigen escape. *Nature* **568**, 112–116 (2019).

11. Olson, M. L. *et al.* Low-affinity CAR T cells exhibit reduced trogocytosis, preventing rapid antigen loss, and increasing CAR T cell expansion. *Leukemia* **36**, 1943–1946 (2022).

12. Li, Y. *et al.* KIR-based inhibitory CARs overcome CAR-NK cell trogocytosis-mediated fratricide and tumor escape. *Nat Med* **28**, 2133–2144 (2022).

13. Camviel, N. *et al.* Both APRIL and antibody-fragment-based CAR T cells for myeloma induce BCMA downmodulation by trogocytosis and internalization. *J. Immunother. Cancer* **10**, e005091 (2022).

14. Marei, H. *et al.* Antibody targeting of E3 ubiquitin ligases for receptor degradation. *Nature* **610**, 182–189 (2022).

15. Békés, M., Langley, D. R. & Crews, C. M. PROTAC targeted protein degraders: the past is prologue. *Nat. Rev. Drug Discov.* **21**, 181–200 (2022).

16. Ruella, M. *et al.* Induction of resistance to chimeric antigen receptor T cell therapy by transduction of a single leukemic B cell. *Nat. Med.* **24**, 1499–1503 (2018).

17. Dixon, A. S. *et al.* NanoLuc Complementation Reporter Optimized for Accurate Measurement of Protein Interactions in Cells. *ACS Chem. Biol.* **11**, 400–408 (2016).

18. Miyake, K. *et al.* Trogocytosis of peptide-MHC class II complexes from dendritic cells confers antigen-presenting ability on basophils. *Proc Natl Acad Sci U S A* **114**, 1111–1116 (2017).

19. Gilmartin, A. A., Ralston, K. S. & Petri, W. A. Inhibition of Amebic Cysteine Proteases Blocks Amebic Trogocytosis but Not Phagocytosis. *J. Infect. Dis.* **221**, 1734–1739 (2020).

20. Reed, J., Reichelt, M. & Wetzel, S. A. Lymphocytes and Trogocytosis-Mediated Signaling. *Cells* **10**, 1478 (2021).

21. Hudrisier, D., Aucher, A., Puaux, A.-L., Bordier, C. & Joly, E. Capture of Target Cell Membrane Components via Trogocytosis Is Triggered by a Selected Set of Surface Molecules on T or B Cells. *J. Immunol.* **178**, 3637–3647 (2007).

22. Cavallo-Medved, D., Moin, K. & Sloane, B. Cathepsin B. *AFCS Nat Mol Pages* **2011**, A000508 (2011).

23. Mort, J. S. & Buttle, D. J. Cathepsin B. *Int. J. Biochem. Cell Biol.* **29**, 715–720 (1997).

24. Vidak, E., Javoršek, U., Vizovišek, M. & Turk, B. Cysteine Cathepsins and Their Extracellular Roles: Shaping the Microenvironment. *Cells* **8**, 264 (2019).

25. Balaji, K. N., Schaschke, N., Machleidt, W., Catalfamo, M. & Henkart, P. A. Surface Cathepsin B Protects Cytotoxic Lymphocytes from Self-destruction after Degranulation. *Journal of Experimental Medicine* **196**, 493–503 (2002).

26. Olson, O. C. & Joyce, J. A. Cysteine cathepsin proteases: regulators of cancer progression and therapeutic response. *Nat Rev Cancer* **15**, 712–729 (2015).

27. Gabrijelcic, D. *et al.* Cathepsins B, H and L in human breast carcinoma. *Eur J Clin Chem Clin Biochem* **30**, 69–74 (1992).

28. Uhlén, M. *et al.* Tissue-based map of the human proteome. *Science* **347**, 1260419 (2015).

29. Estrada, S. *et al.* The Role of Gly-4 of Human Cystatin A (Stefin A) in the Binding of Target Proteinases. Characterization by Kinetic and Equilibrium Methods of the

Interactions of Cystatin A Gly-4 Mutants with Papain, Cathepsin B, and Cathepsin L. *Biochemistry* **37**, 7551–7560 (1998).

30. Pavlova, A., Krupa, J. C., Mort, J. S., Abrahamson, M. & Björk, I. Cystatin inhibition of cathepsin B requires dislocation of the proteinase occluding loop. Demonstration by release of loop anchoring through mutation of His110. *FEBS Lett.* **487**, 156–160 (2000).
31. Pavlova, A. & Björk, I. Grafting of Features of Cystatins C or B into the N-Terminal Region or Second Binding Loop of Cystatin A (Stefin A) Substantially Enhances Inhibition of Cysteine Proteinases. *Biochemistry* **42**, 11326–11333 (2003).
32. Jenko, S. *et al.* Different propensity to form amyloid fibrils by two homologous proteins—Human stefins A and B: Searching for an explanation. *Proteins: Struct., Funct., Bioinform.* **55**, 417–425 (2004).
33. Cohen, A. D. *et al.* B cell maturation antigen-specific CAR T cells are clinically active in multiple myeloma. *J. Clin. Investig.* **129**, 2210–2221 (2019).
34. Radhakrishnan, S. V. *et al.* CD229 CAR T cells eliminate multiple myeloma and tumor propagating cells without fratricide. *Nat. Commun.* **11**, 798 (2020).
35. Grover, P. *et al.* Chimeric antigen receptor T-cell therapy in adults with B-cell acute lymphoblastic leukemia. *Blood Adv* **6**, 1608–1618 (2022).
36. Xu, X. *et al.* Mechanisms of Relapse After CD19 CAR T-Cell Therapy for Acute Lymphoblastic Leukemia and Its Prevention and Treatment Strategies. *Front. Immunol.* **10**, 2664 (2019).

37. Gu, T., Zhu, M., Huang, H. & Hu, Y. Relapse after CAR-T cell therapy in B-cell malignancies: challenges and future approaches. *J. Zhejiang Univ.-Sci. B* **23**, 793–811 (2022).

38. Towatari, T. *et al.* Novel epoxysuccinyl peptides A selective inhibitor of cathepsin B, in vivo. *FEBS Lett.* **280**, 311–315 (1991).

39. Murata, M. *et al.* Novel epoxysuccinyl peptides Selective inhibitors of cathepsin B, in vitro. *FEBS Lett.* **280**, 307–310 (1991).

40. Newick, K., O'Brien, S., Moon, E. & Albelda, S. M. CAR T Cell Therapy for Solid Tumors. *Annu. Rev. Med.* **68**, 139–152 (2016).

41. Sterner, R. C. & Sterner, R. M. CAR-T cell therapy: current limitations and potential strategies. *Blood Cancer J* **11**, 69 (2021).

42. Mause, E. R. V. *et al.* Systematic single amino acid affinity tuning of CD229 CAR T cells retains efficacy against multiple myeloma and eliminates on-target off-tumor toxicity. *Sci. Transl. Med.* **15**, eadd7900 (2023).

43. Lee, D. W. *et al.* T cells expressing CD19 chimeric antigen receptors for acute lymphoblastic leukaemia in children and young adults: a phase 1 dose-escalation trial. *Lancet* **385**, 517–528 (2015).

44. Veatch, S. L. *et al.* Correlation Functions Quantify Super-Resolution Images and Estimate Apparent Clustering Due to Over-Counting. *PLoS ONE* **7**, e31457 (2012).

FIGURE LEGENDS

Figure 1: CAR-mediated trogocytosis directly causes CAR T cell dysfunction. (A) Schema of CAR-mediated trogocytosis (CMT). **(B)** CD19 transfer to CAR T cells lacking an antigen binding domain (ΔscFv) or CD19 CAR T cells (FMC63) after a 1-hour coculture with CD19-positive cell lines at a 0.5:1 effector-target ratio using flow cytometry. **(C)** CD19 loss on tumor cells after a 1-hour coculture with ΔscFv or FMC63 CAR T cells at a 0.5:1 effector-target ratio using flow cytometry. **(D)** Observation of CMT in brightfield and confocal images of ΔscFv or FMC63 CAR T cells cultured with CD19-GFP-expressing 293T cells. CD19 is shown in green. Scale bar represents 5μm. **(E-F)** Amount of CD19 on CAR T cells isolated from patients 7-28 days after receiving CD19 CAR T cell therapy using full-spectrum flow cytometry. Data indicate individual patients. Statistical significance was determined by Wilcoxon matched-pairs signed-rank test. **(G)** Schema of trogocytosed antigen degrader (TAD). **(H)** CD19 and **(I)** GFP expression on FMC63 CAR T cells expressing TAD_{GFP} or T cells expressing a CAR lacking a binding domain (ΔscFv) following a 1-hour coculture with CD19-GFP-expressing NALM6 cells as determined by flow cytometry. **(J)** Schema of a fully human-derived TAD system (TAD_{CD19}). VHL = von Hippel-Lindau protein; Ub = ubiquitin. **(K)** GFP and **(L)** CD19 expression on FMC63 CAR T cells expressing TAD_{CD19} or ΔscFv CAR T cells after a 1-hour coculture with CD19-GFP-expressing NALM6 cells at a 0.5:1 effector-target ratio. **(M)** Quantification of CAR T cells after a 24-hour coculture with CD19-GFP-expressing NALM6 cells using flow cytometry. Values are normalized to wells containing only CAR T cells. **(N)** Expression of LAG-3 and TIM-3 on CAR T cells expressing TAD_{GFP} after a 24-hour coculture with CD19-

GFP-expressing NALM6 cells using full-spectrum flow cytometry. (H-N) Data indicates mean ± S.D. from three technical replicates. Statistical significance was determined by two-tailed Student's *t*-test. **(O)** Schema of *in vitro* serial coculture experiment to determine long-term CAR T cell expansion and antitumor activity. **(P)** Survival of CD19-GFP-expressing NALM6 cells expressing firefly luciferase (Fluc) at a 0.5:1 effector-target ratio using a luminescence-based cytotoxicity assay. Data indicates mean ± S.D. from three technical replicates. Tumor survival was normalized to untreated tumor cells. Statistical significance was determined by multiple *t*-tests and corrected for multiple comparisons using the Bonferroni-Dunn method.

Figure 2: Extracellular cathepsin B is a key driver of CAR-mediated trogocytosis. **(A)** Schema of luciferase complementation assay (CompLuc). **(B)** CMT during coculture of FMC63 CAR T cells expressing nLuc with K562 cells expressing full length or truncated (tr19) CD19 fused to cLuc using CompLuc or flow cytometry after 1 hour at the indicated effector-target ratios. CMT using CompLuc was measured for a total 2.5 hours at 1-minute intervals. Data represents best fit of three technical replicates. **(C)** Area-under-curve quantification of luminescence in Fig. 2B. **(D)** Peak luminescence of FMC63 CAR T cells cocultured with K562 cells expressing CD19-cLuc at a 1:1 effector-target ratio as determined by CompLuc. CAR T cells were pre-treated with cytochalasin D for 1 hour at the indicated concentrations. **(E)** Survival of Raji-Fluc cells after 16-hour coculture with FMC63 CAR T cells pre-treated with the indicated concentrations of cytochalasin D. CMT values are normalized to a DMSO

control. Data represent mean ± S.D. of three technical replicates. **(F)** Schema of potential modulators of CMT. **(G)** Peak luminescence as determined by CompLuc of FMC63 CAR T cells treated with inhibitors of the indicated proteins cocultured with K562 cells expressing CD19-cLuc at a 1:1 effector-target ratio. Values are normalized to a DMSO control. Data represent mean ± S.D. of three technical replicates. **(H)** Survival of Raji-Fluc cells after 16-hour coculture with FMC63 CAR T cells treated with inhibitors of the indicated proteins at a single concentration. Tumor survival was measured using a luciferase-based cytotoxicity assay. Data represent mean ± S.D. of three technical replicates. **(I)** Peak luminescence as determined by CompLuc of FMC63 CAR T cells cocultured with K562 cells expressing CD19-cLuc at a 1:1 effector-target ratio. FMC63 CAR T cells were pre-treated with the indicated concentrations of Ca-074-Me (membrane permeable) or Ca-074 (membrane impermeable). Values are normalized to a DMSO control. Data represent mean ± S.D. of three technical replicates. **(J)** Schema of microscopy setup used to assess cathepsin B (CTSB) localization to the immune synapse. Biotinylated CD19 was immobilized on plate-bound NeutrAvidin. FMC63 CAR T cells expressing CTSB-mCherry were added to slides and imaged using confocal microscopy. **(K)** Side (x-z) view of the distribution of CTSB-mCherry in ΔscFv or FMC63 CAR T cells on immobilized CD19 at indicated time points using spinning disk confocal imaging. **(L)** Axial dispersion of CTSB in fixed ΔscFv and FMC63 CAR T cells 5 minutes after plating. **(M)** Average distance of CTSB to immune synapse in fixed ΔscFv and FMC63 CAR T cells 5 minutes and 15 minutes after plating. (M-N) Statistical significance was determined by two-tailed Student's *t*-test. CMT during coculture of ΔscFv or

FMC63 CAR T cells expressing nLuc with K562 cells expressing CD19-cLuc measured by CompLuc and flow cytometry. CMT using CompLuc was measured for a total 2.5 hours at 1-minute intervals. Flow cytometry was performed immediately following completion of CompLuc. Data represents best fit of three technical replicates.

Figure 3: Expression of human cystatins increases CAR T cell expansion by reducing CTSB-mediated CMT. (A) Crystal structures of bovine cathepsin B in complex with Ca-074 (left, PDB: 1QDQ) and human cathepsin B in complex with cystatin A (right, PDB: 3K9M). The active site cysteine of cathepsin B is shown in pink; Ca-074 and cystatin A are shown in teal. **(B)** Schema of construct used for production of CAR_{CSTA} T cells. **(C)** Levels of CSTA in CAR or CAR_{CSTA} T cells measured by ELISA. Data represent mean ± S.D. of two technical replicates. **(D)** Cathepsin B activity in CAR or CAR_{CSTA} T cells measured by fluorescence. Data represent mean ± S.D. of two technical replicates. **(E)** Expansion of CAR or CAR_{CSTA} CAR T cells during manufacturing as determined by cell counting. **(F)** CAR T cells were analyzed via flow cytometry after production for *(I)* CAR expression, *(II)* T cell subsets, and *(III-IV)* T cell phenotype. **(G)** Survival of Raji-Fluc, NALM6-Fluc, Daudi-Fluc, or Toledo-Fluc cells after 16-hour coculture with FMC63 or CAR_{CSTA} T cells at the indicated effector-target ratios. Tumor survival was measured using a luciferase-based cytotoxicity assay. Data represent mean ± S.D. of three technical replicates. **(H)** CMT and **(I)** area under curve quantification as determined by CompLuc using K562 cells expressing CD19-cLuc after 3 hours. Data represent mean ± S.D. of three technical replicates. **(J)**

CD19 loss on tumor cells, **(K)** CD19 transfer to CAR T cells, and **(L)** total CAR T cells following a 30-minute coculture of FMC63 or CAR_{CSTA} T cells and K562 cells expressing CD19-cLuc at a 0.5:1 effector-target ratio. CAR T cell numbers are normalized to wells containing only CAR T cells using counting beads. Data represent mean ± S.D. of three technical replicates.

Figure 4: Cystatin overexpression improves long-term CAR T cell expansion and efficacy. (A) Schema of in vitro experiment to determine long-term CAR T cell expansion and antitumor activity. **(B)** Quantification of CAR T cells during serial coculture using flow cytometry. CAR T cells were normalized using counting beads. Data represent mean ± S.D. of three technical replicates. **(C)** Mean fluorescence intensity of CD69 in CAR T cells after 24-hour coculture. Data represent mean ± S.D. of three technical replicates. **(D)** Mean fluorescence intensity of Ki67 on Day 5 of serial coculture using flow cytometry. **(E)** Survival of CD19-GFP-expressing NALM6 cells expressing luciferase at a 0.5:1 effector-target ratio using a luminescence-based cytotoxicity assay. Data represent mean ± S.D. of three technical replicates. **(F)** Schema of *in vivo* experiment to measure CAR T cell expansion and persistence. **(G)** Quantification of CAR T cells in murine spleen, peripheral blood, and bone marrow. Statistical significance was determined by two-tailed Student's *t*-test.

Figure 5: CSTA overexpression reduces CMT and increases expansion in BCMA CAR T cells. (A) Schema of various CAR_{BCMA} T cells. **(B)** BCMA transfer to CAR T cells and BCMA loss on BCMA-GFP-expressing K562 cells. **(C)** BCMA loss on MM.1S,

RPMI8226, and U266B1 cells when cocultured with CAR_{BCMA}, Abecma, and Carvykti CAR T cells. **(D)** Expansion of BCMA CAR or CAR_{CSTA} CAR T cells during manufacturing as determined by cell counting. **(E)** BCMA CAR T cells were analyzed via flow cytometry after production for *(I)* CAR expression, *(II)* T cell subsets, and *(III-IV)* T cell phenotype. **(F)** Survival of MM.1S-, RPMI8226-, and U266B1-Fluc cells after 16-hour coculture with BCMA CAR or CAR_{CSTA} T cells at the indicated effector-target ratios. Tumor survival was measured using a luciferase-based cytotoxicity assay. Data represent mean ± S.D. of three technical replicates. **(G)** BCMA CAR T cell expansion after 16-hour coculture with the indicated tumor cell lines at an 8:1 effector-target ratio. **(H)** CMT and **(I)** area under curve quantification as determined by CompLuc using K562 cells expressing BCMA-GFP-cLuc after 3 hours. Data represent mean ± S.D. of three technical replicates. **(J)** BCMA loss on U266B1 tumor cells after 2-hour coculture with BCMA CAR or CAR_{CSTA} T cells. **(K)** BCMA-GFP transfer to CAR T cells, and **(L)** total CAR T cells following a 30-minute coculture of BCMA CAR or CAR_{CSTA} T cells and K562 cells expressing CD19-cLuc at a 1:1 effector-target ratio. CAR T cell numbers are normalized to wells containing only CAR T cells using counting beads. (H-L) Data represent mean ± S.D. of three technical replicates. (G, I-L) Statistical significance was determined by two-tailed Student's *t*-test.

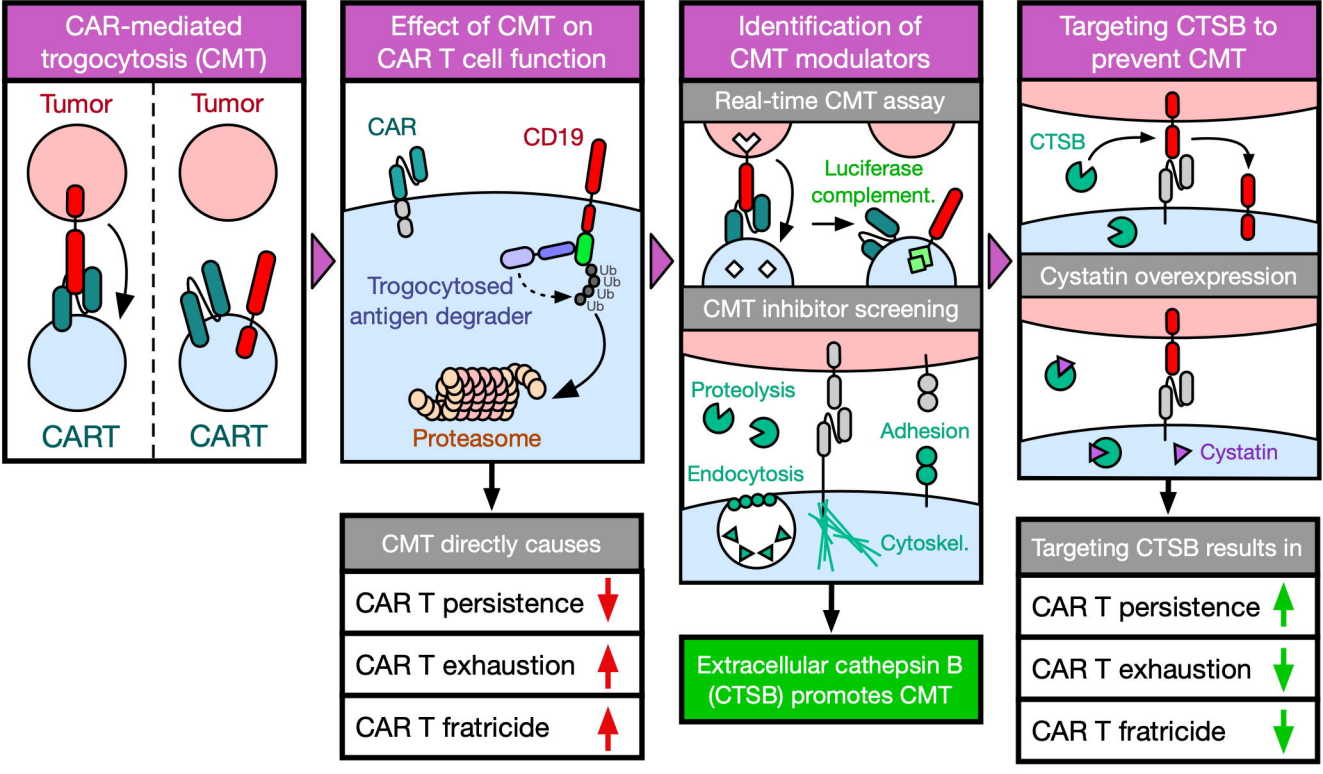
CAR-mediated trogocytosis (CMT)
Tumor
Tumor
CART
CART
Effect of CMT on CAR T cell function
CAR
CD19
Ub
Ub
Ub
Ub
Trogocytosed antigen degrader
Proteasome
CMT directly causes
CAR T persistence
CAR T exhaustion
CAR T fratricide
Identification of CMT modulators
Real-time CMT assay
Luciferase complement.
CMT inhibitor screening
Proteolysis
Adhesion
Endocytosis
Cytoskel.
Extracellular cathepsin B (CTSB) promotes CMT
Targeting CTSB to prevent CMT
CTSB
Cystatin overexpression
Cystatin
Targeting CTSB results in
CAR T persistence
CAR T exhaustion
CAR T fratricide

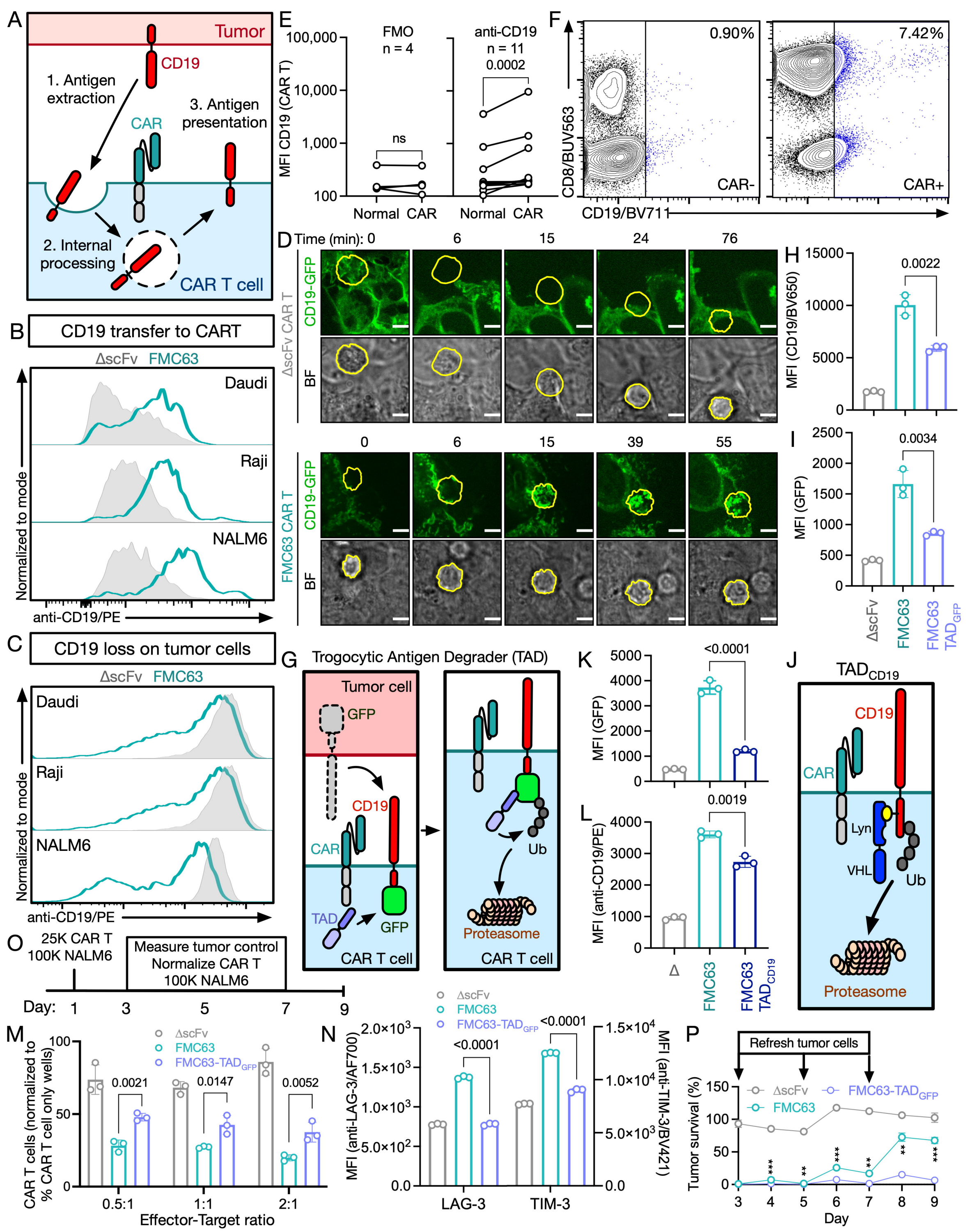
A
Tumor
CD19
1. Antigen extraction
CAR
3. Antigen presentation
2. Internal processing
CAR T cell
B
CD19 transfer to CART
ΔscFv FMC63
Daudi
Raji
NALM6
Normalized to mode
anti-CD19/PE
C
CD19 loss on tumor cells
ΔscFv FMC63
Daudi
Raji
NALM6
Normalized to mode
anti-CD19/PE
E
FMO
n = 4
anti-CD19
n = 11
0.0002
ns
MFI CD19 (CAR T)
100,000
10,000
1,000
100
Normal CAR
Normal CAR
F
0.90%
7.42%
CD8/BUV563
CD19/BV711
CAR-
CAR+
D
Time (min): 0 6 15 24 76
ΔscFv CAR T
CD19-GFP
BF
0 6 15 39 55
FMC63 CAR T
CD19-GFP
BF
H
MFI (CD19/BV650)
15000
10000
5000
0
0.0022
I
MFI (GFP)
2500
2000
1500
1000
500
0
0.0034
ΔscFv
FMC63
FMC63 TAD$_{GFP}$
G
Trogocytic Antigen Degrader (TAD)
Tumor cell
GFP
CD19
CAR
TAD
GFP
CAR T cell
Ub
Proteasome
CAR T cell
K
MFI (GFP)
5000
4000
3000
2000
1000
0
<0.0001
0.0019
L
MFI (anti-CD19/PE)
4000
3000
2000
1000
0
Δ
FMC63
FMC63 TAD$_{CD19}$
J
TAD$_{CD19}$
CD19
CAR
Lyn
VHL
Ub
Proteasome
O
25K CAR T
100K NALM6
Measure tumor control
Normalize CAR T
100K NALM6
Day: 1 3 5 7 9
M
ΔscFv
FMC63
FMC63-TAD$_{GFP}$
CAR T cells (normalized to % CAR T cell only wells)
100
50
0
0.0021
0.0147
0.0052
0.5:1
1:1
2:1
Effector-Target ratio
N
ΔscFv
FMC63
FMC63-TAD$_{GFP}$
MFI (anti-LAG-3/AF700)
2.0×10^3
1.5×10^3
1.0×10^3
5.0×10^2
0.0
<0.0001
<0.0001
MFI (anti-TIM-3/BV421)
1.5×10^4
1.0×10^4
5.0×10^3
0.0
LAG-3
TIM-3
P
Refresh tumor cells
ΔscFv
FMC63
FMC63-TAD$_{GFP}$
Tumor survival (%)
150
100
50
0
***
**
***
**
**
***
3 4 5 6 7 8 9
Day

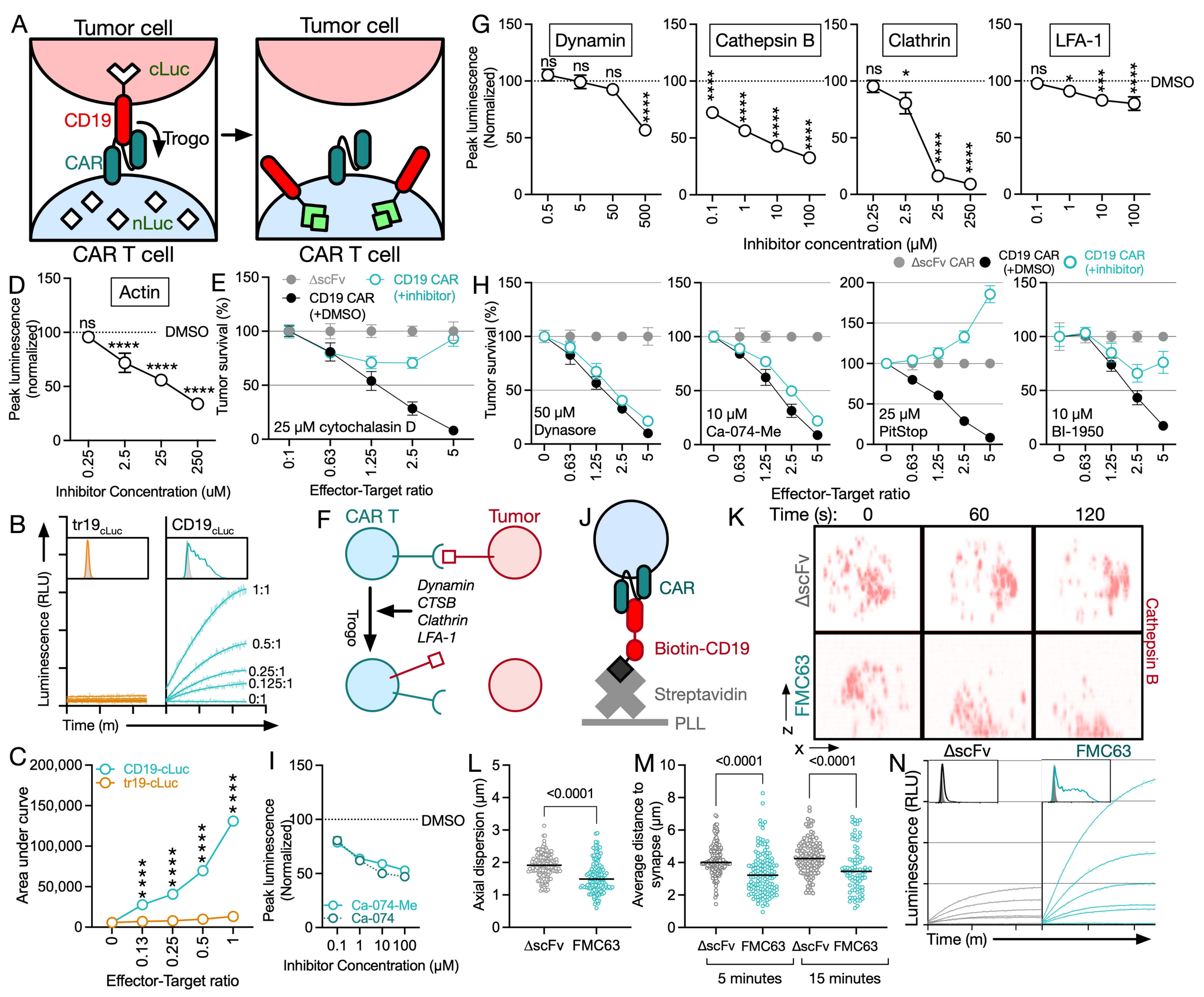
A
Tumor cell
cLuc
CD19
Trogo
CAR
nLuc
CAR T cell
Tumor cell
CAR T cell
G
Dynamin
Cathepsin B
Clathrin
LFA-1
Peak luminescence (Normalized)
ns
****
*
DMSO
Inhibitor concentration (μM)
D
Actin
Peak luminescence (normalized)
Inhibitor Concentration (uM)
E
ΔscFv
CD19 CAR (+DMSO)
CD19 CAR (+inhibitor)
Tumor survival (%)
25 μM cytochalasin D
Effector-Target ratio
H
50 μM Dynasore
10 μM Ca-074-Me
25 μM PitStop
10 μM BI-1950
B
tr19cLuc
CD19cLuc
Luminescence (RLU)
1:1
0.5:1
0.25:1
0.125:1
0:1
Time (m)
F
CAR T
Tumor
Dynamin
CTSB
Clathrin
LFA-1
Trogo
J
CAR
Biotin-CD19
Streptavidin
PLL
K
Time (s): 0 60 120
ΔscFv
FMC63
Cathepsin B
z
x
C
CD19-cLuc
tr19-cLuc
Area under curve
Effector-Target ratio
I
Peak luminescence (Normalized)
DMSO
Ca-074-Me
Ca-074
Inhibitor Concentration (μM)
L
Axial dispersion (μm)
<0.0001
ΔscFv FMC63
M
Average distance to synapse (μm)
<0.0001
<0.0001
ΔscFv FMC63 ΔscFv FMC63
5 minutes
15 minutes
N
ΔscFv
FMC63
Luminescence (RLU)
Time (m)

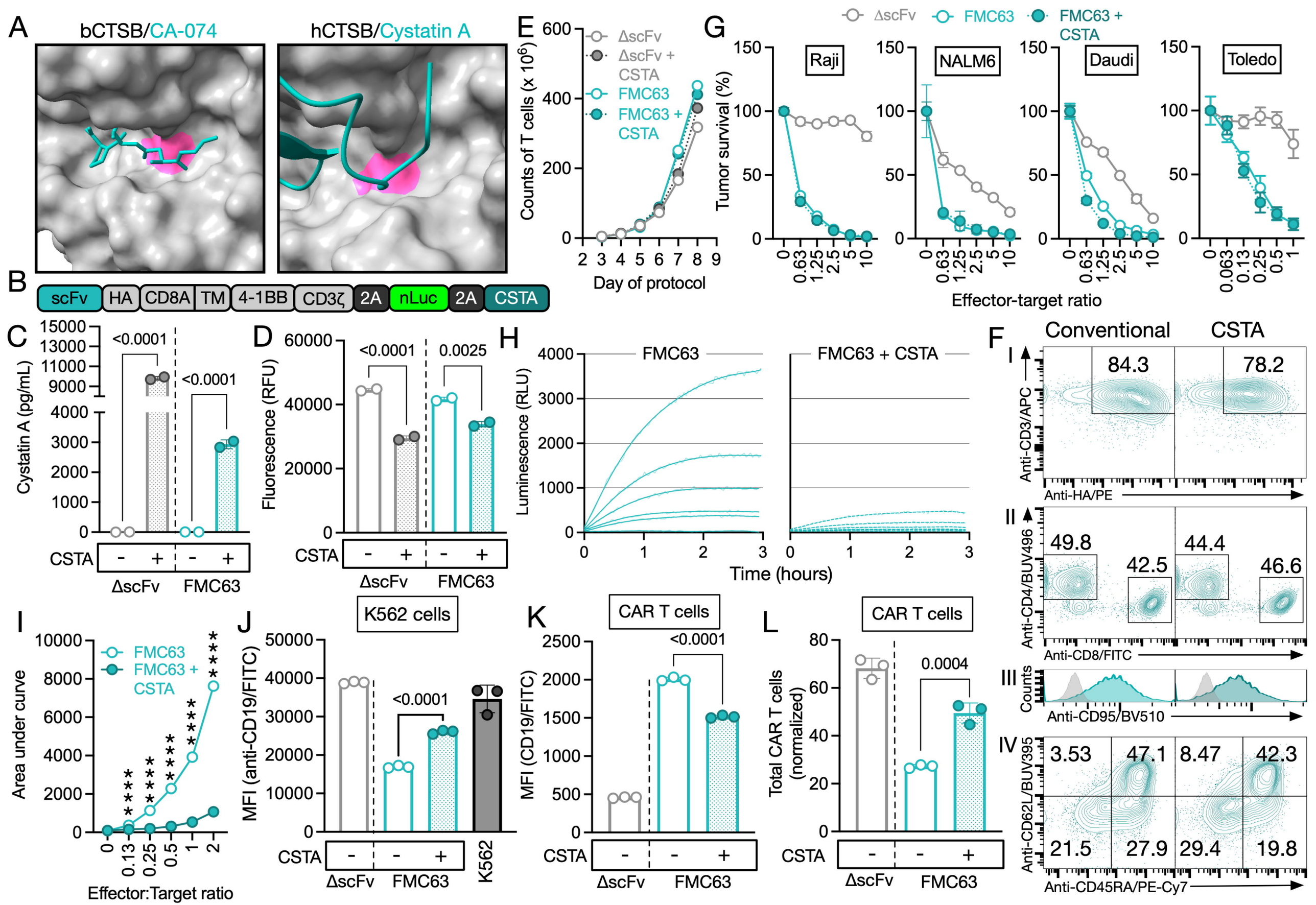
A
bCTSB/CA-074
hCTSB/Cystatin A
B
scFv
HA
CD8A
TM
4-1BB
CD3ζ
2A
nLuc
2A
CSTA
C
Cystatin A (pg/mL)
<0.0001
<0.0001
CSTA
ΔscFv
FMC63
D
Fluorescence (RFU)
<0.0001
0.0025
CSTA
ΔscFv
FMC63
E
Counts of T cells (x 10^6)
ΔscFv
ΔscFv + CSTA
FMC63
FMC63 + CSTA
Day of protocol
G
ΔscFv
FMC63
FMC63 + CSTA
Raji
NALM6
Daudi
Toledo
Tumor survival (%)
Effector-target ratio
H
FMC63
FMC63 + CSTA
Luminescence (RLU)
Time (hours)
F
Conventional
CSTA
84.3
78.2
Anti-CD3/APC
Anti-HA/PE
49.8
42.5
44.4
46.6
Anti-CD4/BUV496
Anti-CD8/FITC
Counts
Anti-CD95/BV510
3.53
47.1
8.47
42.3
21.5
27.9
29.4
19.8
Anti-CD62L/BUV395
Anti-CD45RA/PE-Cy7
I
FMC63
FMC63 + CSTA
Area under curve
Effector:Target ratio
J
K562 cells
MFI (anti-CD19/FITC)
<0.0001
CSTA
ΔscFv
FMC63
K562
K
CAR T cells
MFI (CD19/FITC)
<0.0001
CSTA
ΔscFv
FMC63
L
CAR T cells
Total CAR T cells (normalized)
0.0004
CSTA
ΔscFv
FMC63

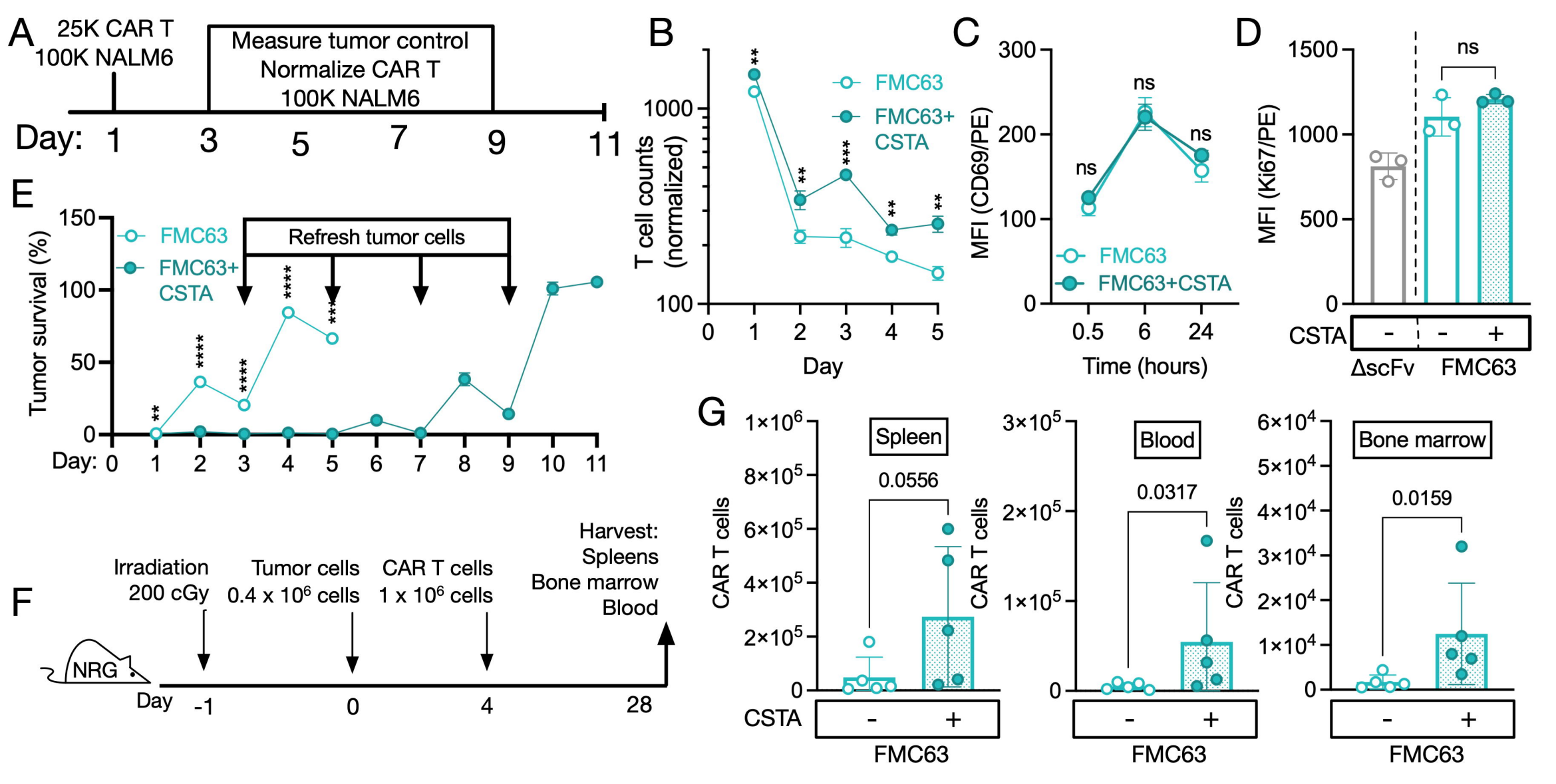
A
25K CAR T
100K NALM6
Measure tumor control
Normalize CAR T
100K NALM6
Day: 1 3 5 7 9 11
B
T cell counts (normalized)
FMC63
FMC63+ CSTA
Day
C
MFI (CD69/PE)
ns
FMC63
FMC63+CSTA
Time (hours)
D
MFI (Ki67/PE)
ns
CSTA
ΔscFv
FMC63
E
Tumor survival (%)
FMC63
FMC63+ CSTA
Refresh tumor cells
Day:
F
Irradiation 200 cGy
Tumor cells 0.4 x 10^6 cells
CAR T cells 1 x 10^6 cells
Harvest: Spleens Bone marrow Blood
NRG
Day -1 0 4 28
G
Spleen
Blood
Bone marrow
CAR T cells
0.0556
0.0317
0.0159
CSTA
FMC63

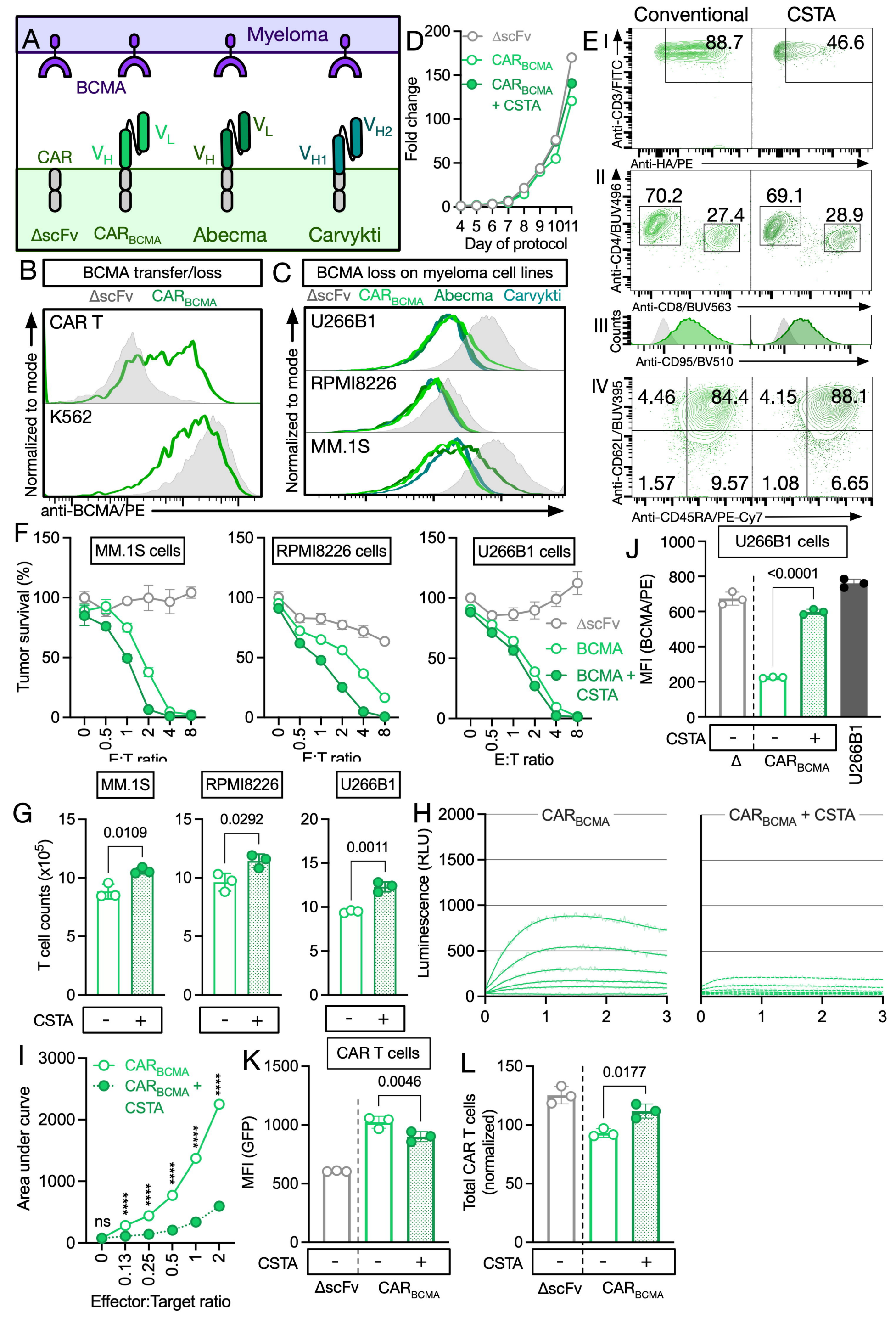
A
Myeloma
BCMA
CAR
V_H
V_L
V_{H1}
V_{H2}
ΔscFv
CAR_{BCMA}
Abecma
Carvykti
B
BCMA transfer/loss
ΔscFv
CAR_{BCMA}
CAR T
K562
Normalized to mode
anti-BCMA/PE
C
BCMA loss on myeloma cell lines
ΔscFv
CAR_{BCMA}
Abecma
Carvykti
U266B1
RPMI8226
MM.1S
Normalized to mode
D
ΔscFv
CAR_{BCMA}
CAR_{BCMA} + CSTA
Fold change
Day of protocol
E
Conventional
CSTA
I
88.7
46.6
Anti-CD3/FITC
Anti-HA/PE
II
70.2
27.4
69.1
28.9
Anti-CD4/BUV496
Anti-CD8/BUV563
III
Counts
Anti-CD95/BV510
IV
4.46
84.4
4.15
88.1
1.57
9.57
1.08
6.65
Anti-CD62L/BUV395
Anti-CD45RA/PE-Cy7
F
MM.1S cells
RPMI8226 cells
U266B1 cells
Tumor survival (%)
E:T ratio
ΔscFv
BCMA
BCMA + CSTA
J
U266B1 cells
<0.0001
MFI (BCMA/PE)
CSTA
Δ
CAR_{BCMA}
U266B1
G
MM.1S
RPMI8226
U266B1
0.0109
0.0292
0.0011
T cell counts (x10^5)
CSTA
H
CAR_{BCMA}
CAR_{BCMA} + CSTA
Luminescence (RLU)
I
CAR_{BCMA}
CAR_{BCMA} + CSTA
ns
****
Area under curve
Effector:Target ratio
K
CAR T cells
0.0046
MFI (GFP)
CSTA
ΔscFv
CAR_{BCMA}
L
0.0177
Total CAR T cells (normalized)
CSTA
ΔscFv
CAR_{BCMA}